High efficiency SNG production from biomass and electricity by integrating gasification with pressurized solid oxide electrolysis cells

Clausen, Lasse R.; Butera, Giacomo; Jensen, Søren Højgaard

Published in:
Energy

Link to article, DOI:
10.1016/j.energy.2019.02.039

Publication date:
2019

Document Version
Peer reviewed version

High efficiency SNG production from biomass and electricity by integrating gasification with pressurized solid oxide electrolysis cells

Lasse R. Clausen[1,*], Giacomo Butera[1], Søren Højgaard Jensen[2]

[1] Section of Thermal Energy, Department of Mechanical Engineering, Technical University of Denmark (DTU), Nils Koppels Allé Bld. 403, 2800 Kgs. Lyngby, Denmark

[2] DTU Energy, Technical University of Denmark, Frederiksborgvej 399, 4000 Roskilde, Denmark

Received: xx

Abstract

Co-electrolysis of CO_2 and H_2O in pressurized solid oxide electrolysis cells (SOEC) results in internal methanation when the fuel electrode contains nickel, as nickel catalyzes the methanation reaction. Recent SOEC stack experiments operated at 19 bar and 700°C produced a gas with a methane content of 18 vol% (dry). The exothermic methanation reaction is a perfect match for the endothermic electrolysis reactions, enabling an overall slightly exothermic stack operation at a moderate polarization voltage. When using a pressurized SOEC for biomass syngas upgrading to synthetic natural gas, it is possible to achieve very high energy efficiency because a high share of the exothermic methane formation can occur inside the SOEC. The production of waste heat from the downstream methanation reactor is therefore reduced significantly. In this paper, such an integrated system design is proposed and evaluated by thermodynamic modelling and analysis. The analysis shows that the proposed system can reach 84% energy efficiency from wood pellets and electricity to synthetic natural gas. This is substantially higher than the ~70% efficiency than can be achieved with steam electrolysis based systems. If steam drying is integrated to allow the use of wet wood chips, the efficiency drops to 82%.

Keywords: gasification, electrolysis, SOEC, internal methanation, synthetic natural gas, thermodynamic analysis.

Nomenclature

Symbols		*Abbreviations*	
ASR	Area specific resistance [$\Omega \cdot cm^2$]	AC	Alternating current
E	Nernst voltage [V]	ASR	Area specific resistance
F	Faraday constant	COP	Coefficient of performance
g	Specific Gibbs free energy	DC	Direct current
G	Gibbs free energy	DME	Dimethyl ether
i	Current density [A/cm^2]	DNA	Dynamic Network Analysis
I	Current [A]	LHV	Lower heating value
$\dot{m}$	Mass flow rate [kg/s]	LT	Low temperature
M	Gas module	SNG	Synthetic natural gas
$\dot{n}$	Molar flow rate [kmol/s]	SOEC	solid oxide electrolysis cell
$\dot{Q}$	Heat flow [MW]	SOFC	solid oxide fuel cell
V	Voltage [V]		
		Greek letters	
		Δ	Change
		η	Efficiency

*Corresponding author. Tel.: +45 20712778; fax: +45 45884325. E-mail address: lrc@mek.dtu.dk (L.R. Clausen).

1. Introduction

Pressurized operation of solid oxide electrolysis cells (SOEC) with internal methanation is a relatively new field of study. Very few papers have been published on the theoretical potential of these systems and even fewer experimental studies have been published. State of the art within experimental studies includes the paper by Jensen et al. [1] showing that internal methanation occurs at 19 bar when operating an SOEC stack at 700 °C on CO_2 and H_2O. The methane content in the exit gas was measured to 18 vol% (dry) at a specific operating point, which was close to what chemical equilibrium predicted. That the methane content can be predicted by chemical equilibrium has also been demonstrated at atmospheric pressure [2]. Pressurized operation of SOEC's have also been demonstrated by Momma et al. [3]. State of the art within theoretical studies includes the work by Wendel et al. [4], Jensen et al. [5] and Giacomo et al [6]. These three studies concern electricity storage systems based on pressurized reversible SOEC's. In [4,5], the electricity is stored as a methane rich gas in a dedicated cavern or tank, while in [6], electricity is stored as synthetic natural gas (SNG) directly on the natural gas grid. In the paper by Giacomo et al., it is shown that the storage efficiency is increased when storing electricity as pure methane (SNG) instead of a methane rich gas. The efficiency from electricity to SNG is calculated to be 89% (LHV) [6], and the storage efficiency (from electricity to electricity) is calculated to be 80% (DC to DC).

When integrating electrolysis and biomass gasification it is possible to achieve almost full conversion of the biomass carbon to biofuel typically by adding electrolytic hydrogen to the biomass syngas before biofuel synthesis [7–11]. Such a system can act as a flexible demand to balance renewable electricity production from e.g. wind and solar, and furthermore provide an indirect electrification of the transportation sectors where direct electrification is difficult, such as aviation, shipping and heavy goods transport. Studies about integration of electrolysis and gasification of biomass for the production of SNG include [8,9,11]. All of these studies use separate steam electrolysis as illustrated in Fig. 1, where hydrogen is produced by water/steam electrolysis and then mixed with syngas from a gasifier before synthesis of SNG. This type of system will serve as a reference system for comparison with the new type of system we present in this paper. We will refer to the reference type systems as a "steam electrolysis" system.

In [10], a gasifier and an SOEC is connected in series, meaning that electrolysis is performed on a syngas from a gasifier, but this is at atmospheric pressure, which means that internal methanation does not occur to a significant extent. The generated syngas from the SOEC is in that case used for production of Dimethyl ether (DME) [10]. There are currently no studies examining the integration of gasification with pressurized SOEC's conducting internal methanation. The purpose of this paper is therefore to present a design for such a system producing SNG, and to analyze the system by thermodynamic modelling and compare it with a state-of-the-art plant using steam electrolysis (Fig. 1). To distinguish between the two types of systems, we will refer to the new system as an "electrocatalysis" system as it conducts electrolysis on both H_2O and CO_2, as well as catalytic formation of CH_4 from the produced H_2 and CO. Simplified flowsheets of both systems can be seen in Fig. 2 and Fig. 1. An obvious difference between the two systems is that by using steam electrolysis, the generated syngas can be used for synthesis of many different fuels or chemicals, but when the gasifier and SOEC operate in series at elevated pressure (Fig. 2), the fuel gas from the SOEC will have a high methane content, and is therefore mainly suited for SNG production. By comparing the two figures, it can be seen that the steam electrolysis system includes biomass drying while the electrocatalysis system does not. There is simply not enough waste heat from the methanation reactor to include biomass drying in the new system. This is because that most of the exothermic methanation reactions occur inside the SOEC. In both systems (Fig. 1 and Fig. 2), steam is used as sweep gas on the oxygen electrode to lower the oxygen partial pressure and to ease oxygen handling and injection to the gasifier. Using steam as sweep gas for an SOEC has been demonstrated by Barelli et al. [12]. However, long term tests have to be performed to evaluate any

degradation issues. This is also true for pressurized operation of SOEC's. In the proposed system (Fig. 2), the syngas from the gasifier is split before the SOEC in order to 1) allow for a high H/C ratio in the SOEC with a minimum steam injection requirement - a high H/C ratio is needed to avoid carbon formation, and 2) being able to inject a carbon rich gas before the downstream methane reactor to enable conversion of the excess hydrogen present in the gas from the SOEC.
To summarize, in this paper a design for an integrated gasifier and pressurized SOEC "electrocatalysis"-based system is presented (Fig. 2) and analyzed by thermodynamic modelling, calculating energy flows and energy efficiencies. The results are compared with thermodynamic modeling of a state-of-the-art "steam electrolysis"-based system (Fig. 1).

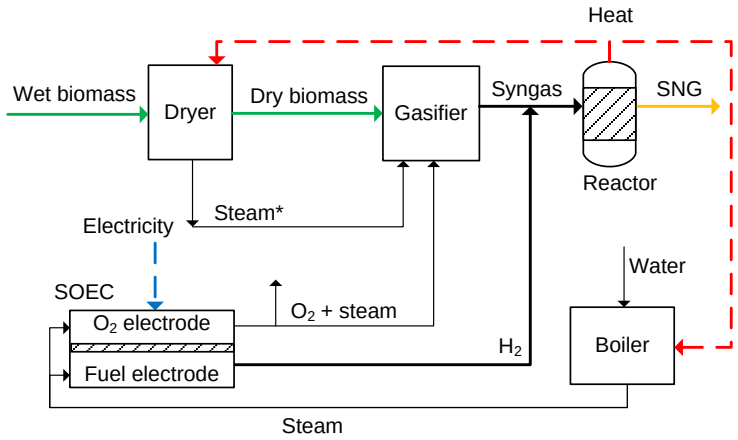

Fig. 1. Simplified flowsheet of a state-of-the-art system for integration of steam electrolysis and biomass gasification for SNG production. *only if a steam dryer is used.

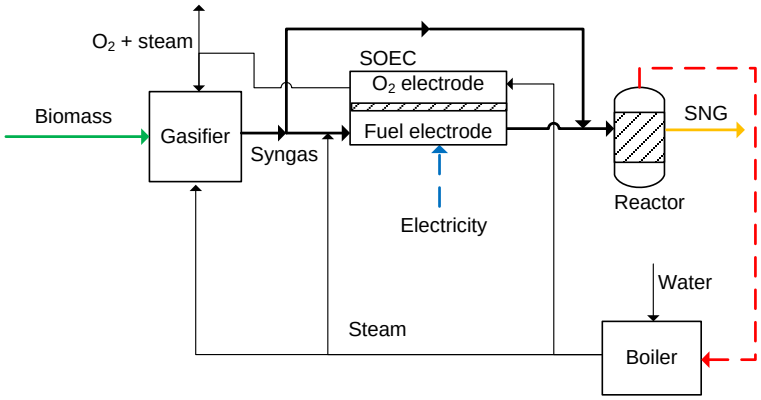

Fig. 2. Simplified flowsheet of the proposed design integrating pressurized SOEC and biomass gasification for SNG production.

2. Design and modelling of the SNG plant

The design of the SNG plant is based on the design of the electricity storage system by Giacomo et al. mentioned above [6]. The main difference between the two plants is that the carbon input for the present plant is generated by a biomass gasifier, while the carbon input for the system presented by Giacomo et al. is a CO_2 rich gas generated by operation of the system in SOFC mode.
A flowsheet of the SNG plant showing all the important processing equipment is provided in the results section. The first step in the plant is the conversion of wood pellets to syngas by pressurized thermal gasification. The gasifier is discussed in detail in the next section. It generates a syngas almost free of tar

compounds, which eliminates the need for tar removal. The syngas is cleaned for particles, dried, compressed and then cleaned for sulfur in a guard bed consisting of metal oxides such as ZnO and CuO [13]. The syngas drying ensures an efficient H_2S removal in the guard bed, because H_2O is a byproduct of the H_2S reaction with metal oxides (eq. 1) [13,14].

$$ZnO + H_2S \leftrightarrow ZnS + H_2O \qquad -76.1\ kJ \qquad (1)$$

The clean and dry syngas is then split in two flows. The main flow goes to a humidifier, while the remaining gas is injected downstream the SOEC. The main syngas flow is humidified by injection of hot water coming from a condenser. This humidifier-condenser loop is a simple system that is able to provide a significant amount of the steam needed to increase the syngas H/C ratio before the SOEC. This reduces the heat requirement of the conventional steam generator. The H/C ratio needs to be sufficiently high to avoid carbon formation in the SOEC [6]. After injection of steam from the steam generator, the gas is preheated in an adiabatic methanator. The hot gas enters the SOEC and oxygen is transferred as oxide ions from the fuel electrode of the SOEC to the oxygen electrode. This oxygen removal together with the high pressure moves the chemical equilibrium towards higher methane content, and because the methanation reaction is catalyzed by the nickel in the fuel electrode, a substantial part of the CO and CO_2 in the gas is converted to methane. The hot methane rich gas exits the SOEC and is then mixed with the upstream residual syngas flow. The resulting gas composition of H_2, CO and CO_2 is optimized for the methane synthesis. After the cooled low temperature (LT) methanator, the gas consists primarily of methane and steam. The steam content is removed by the condenser and residual water vapor is removed by an absorbent before injection to the natural gas grid.
The medium pressure steam raised by cooling the low temperature methanator is used for three purposes: 1) injection to the fuel gas before the SOEC, 2) as motive steam for an ejector used in the gasifier system, and 3) as motive steam for an ejector used on the oxygen side of the SOEC. The steam used by the ejector on the oxygen side of the SOEC has two purposes besides being the motive flow: 1) it provides the needed cooling of the SOEC, 2) it dilutes the oxygen to ease handling, reduces oxygen cross-over in the SOEC, and decreases the Nernst potential. The easier handling of the oxygen-steam mixture includes gasifier injection and turbine expansion of the excess oxygen produced.
In the paragraphs below further information is provided about the main components used.
The system was designed and modelled in the in-house modeling tool DNA (Dynamic Network Analysis) [15,16]. DNA is a component based zero-dimensional thermodynamic modelling and simulation tool that automatically includes conservation of mass and energy.

Gasification

A new design of the TwoStage Gasifier is used for the conversion of biomass to clean syngas. The new design has the same key advantages as the original design [17], which are 1) high cold gas efficiency and, 2) very low tar content in the produced syngas, making tar removal unnecessary [17]. The new design has several advantages compared with the original design, exemplified by the pilot plant called the "Viking gasifier" [18]. The new design uses two updraft fixed beds, one for pyrolysis and one for char gasification (Fig. 3), whereas the Viking gasifier uses a heated screw conveyer for pyrolysis and a downdraft fixed bed for char gasification. The key advantage of updraft fixed beds is that the plant is much easier to scale up. It is estimated that the original design could be scaled to ~10 MWth input whereas the new design can be scaled to 50-100 MWth input[1]. An updraft fixed bed char reactor is also

[1] These values are for atmospheric pressure. When pressurized, it is expected that the new design will be able to handle even more thermal input. As a conservative estimate the thermal input is kept at 100 MWth for the pressurized design used in this paper.

much more tolerant with regards to fines compared with a downdraft fixed bed, making it possible to use lower quality wood chips and various pelletized fuels. The disadvantage of the updraft char reactor is that the inlet gas temperature has to be restricted to ~950°C because of the metal grate in the bottom of the reactor, but also to avoid agglomeration of the ash on the grate. To achieve this, recirculation of syngas by an ejector is used (Fig. 3). Gas recirculation is also used on the pyrolysis reactor where a lower operating temperature allows the use of a gas blower. The recirculation of pyrolysis gasses has two main advantages: 1) it avoids dilution of the pyrolysis gas with e.g. steam, enabling an efficient tar removal by partial oxidation (POX) because of the high temperature achieved by the undiluted pyrolysis gas, 2) enables the utilization of the sensible heat of the syngas for pyrolysis heating and preheating before partial oxidation (Fig. 3). Construction of a small-scale updraft pyrolysis reactor, incl. gas recirculation, has just been finalized. This new design of the TwoStage gasifier is similar to a design presented in [19], where the updraft char gasifier is replaced by a fluid bed. Pressurized updraft fixed bed gasification has been commercially proven by the Lurgi Fixed Bed Dry Bottom Gasifier on coal. There is approximately 150 operating gasifiers of this type in the world according to The National Energy Technology Laboratory (NETL) [20]. The gasifier has an operating pressure of up to 40 bar [21] and a bottom grate temperature of about 980°C (1800°F) [20]. The size of the gasifier is up to 60 ton coal per hour, which corresponds to approx. 500 MWth input [22].

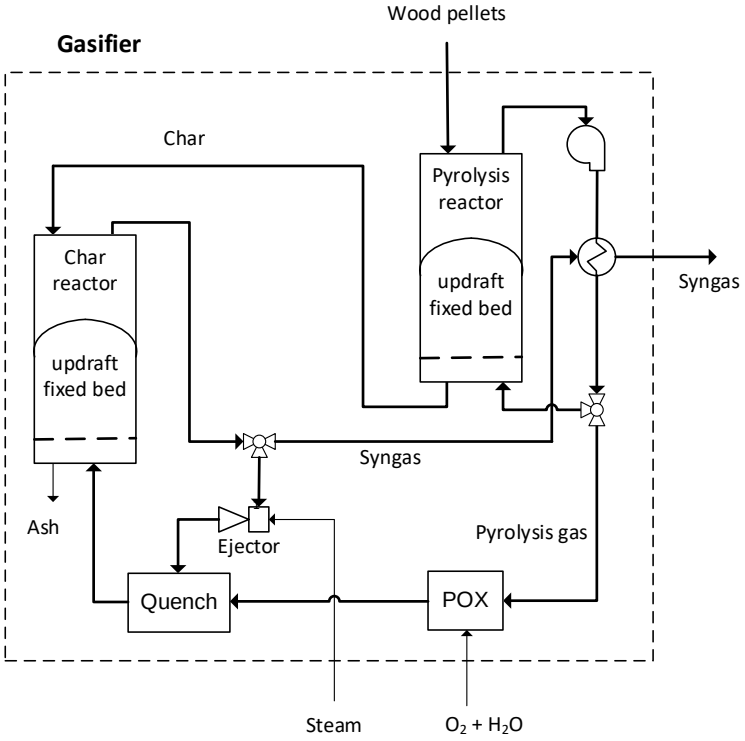

Fig. 3. Detailed flowsheet of the gasifier.

SOEC

Solid oxide electrolysis cells (SOEC) are mainly used for conversion of H_2O to H_2 and O_2 by consumption of electricity, but an SOEC can also convert CO_2 to CO [23]. Combined electrolysis of H_2O and CO_2 is referred to as co-electrolysis, and when co-electrolysis is performed in a pressurized SOEC, some of the produced CO and H_2 will react to form methane catalyzed by the nickel content of the fuel electrode [1,2,5]. The exothermic methanation reaction is a perfect match for the endothermic electrolysis reactions, typically resulting in an overall slightly exothermic stack operation [4,5]. The fuel gas leaving

the SOEC is assumed to be in chemical equilibrium, which is in line with experiments performed at atmospheric pressure [2], but also in line with experiments performed at 19 bar [1].
The operating cell voltage of the zero dimensional SOEC model is calculated by assuming a constant area specific resistance (ASR) and using eq. (1). The average Nernst potential used in this equation is calculated by eq. (2), which is a modified version of the definition of the Nernst potential (eq. (3)). The definition of the Nernst potential (eq. (3)) is modified by multiplying both the numerator and the denominator with the molar flow. The $\dot{\Delta G}$ is calculated by eq. (4). The considered gas flows for the stack model is co-flow and counter-flow where the air-side and fuel-side gasses either flow in the same or opposite direction. For further details on the modelling of the SOEC please see [6].

$$V_{SOEC} = E_{Nernst,average} - ASR \cdot i_{SOEC} \quad (1)$$

$$E_{Nernst,average} = \frac{\dot{\Delta G}}{I_{SOEC}} \quad (2)$$

$$E_{Nernst} = -\frac{\Delta G}{n_e \cdot F} \quad (3)$$

$$\dot{\Delta G} = \dot{m}_{fuel,IN}\, g_{fuel,IN} + \dot{m}_{air,IN}\, g_{air,IN} + \dot{m}_{fuel,OUT}\, g_{fuel,OUT} + \dot{m}_{air,OUT}\, g_{air,OUT} \quad (4)$$

Where i_{SOEC} is the current density, I_{SOEC} is the total current, ΔG is the change in Gibbs free energy of a general electrochemical reaction, n_e the number of electrons transferred during the reaction and F the Faraday constant. $\dot{m}$ is the mass flow and g is the specific Gibbs free energy. It is important that the specific Gibbs free energies used in eq. (4) are calculated at the exit temperature (700°C). The model of the SOEC therefore assumes an isothermal SOEC.
It should be noted that the SOEC system does not include recuperative heat exchangers to preheat input gas to the fuel or oxygen side. Recuperative heat exchangers are very common for SOEC and SOFC systems, but due to the pressurization of the SOEC and the use of syngas as feed, it is possible to make a design without recuperative heat exchangers. The inlet gas to the oxygen side is preheated by recycling some of the hot oxygen rich gas from the SOEC with an ejector. The inlet gas to the fuel side of the SOEC is preheated by an adiabatic methanator. Because recuperative heat exchangers could represent a considerable capital cost, it is estimated that the proposed SOEC system design could be less expensive. From an energy efficiency point of view the proposed design can be more efficient than a design with recuperative heat exchangers. This is because the excess steam-oxygen gas from the SOEC (the part of the flow not recycled or sent to the gasifier) can be expanded in a turbine from the operating temperature of the SOEC (700°C). With recuperative heat exchangers, the gas has to be expanded from the lower outlet temperature of the heat exchanger.

Methanation reactors
Two types of methanation reactors are used in the SNG plant. The main reactor is a boiling water reactor operating at 280°C, in which the excess hydrogen present in the methane rich gas from the SOEC is converted to methane by injection of a carbon rich gas just before the reactor. The carbon rich gas is in this plant simply a fraction of the gasifier syngas bypassing the SOEC. The gas flow rates are selected such that the gas module M (eq. (5)) is set equal to three, which is a value that can be extracted from the chemical reaction equations (eq. (6) and (7)). After the boiling water reactor and after water removal, the methane content is sufficiently high for direct injection to the natural gas grid.
The second methanation reactor used in the SNG plant is an adiabatic reactor used to preheat the fuel gas to the SOEC. Using an adiabatic reactor instead of a heat exchanger to reach an appropriate inlet temperature to the SOEC has three advantages: 1) a recuperative heat exchanger is avoided, the hot outlet gas from the SOEC can then be used to superheat steam and thereafter to raise steam in the boiling water reactor, and 2) the input gas to the SOEC is very close to equilibrium, which can be

important to reduce thermal stresses in the SOEC inlet due to methanation reactions, 3) the SOEC will be less exothermal thus reducing the cooling need, which is covered by injection of saturated steam on the oxygen side of the SOEC (via the ejector).

$$M = \frac{H_2 - CO_2}{CO + CO_2} \quad (5)$$

$CO + 3H_2 \leftrightarrow CH_4 + H_2O$ -206 kJ (6)

$CO_2 + 4H_2 \leftrightarrow CH_4 + 2H_2O$ -165 kJ (7)

Table 1

Process design parameters used in the modeling.

Feedstock	Wood pellets. The dry composition is assumed to be (wt%): 48.1% C, 6.4% H, 44.8% O, 0.1% N, 0.6% ash [19]. The sulfur content is neglected[a]. Water content = 7 wt%. LHV = 18.28 MJ/kg_{dry}. c_p = 1.35 kJ/(kg_{dry}*K). The biomass input is 100 MWth (LHV dry).
Gasifier	P_{out} = 19 bar. Carbon conversion = 99%. Heat loss = 2% of the biomass thermal input (LHV dry). T_{exit} char reactor = 750°C. T_{exit} pyrolysis reactor = 700°C. The gas (excl. CH_4) is assumed to be in chemical equilibrium at the outlet of the char reactor (750°C). CH_4 content of dry syngas = 0.01 mole%[b]. c_p of ash = 1 kJ/(kg*K). Pressure loss of each fixed bed reactor = 300 mbar.
SOEC	Inlet temperature on both fuel and oxygen side = 614°C[c]. Operating/exit temperature = 700°C. operating pressure = 20 bar. Pressure loss = 30 mbar [4]. 10% H_2O+CO_2 in outlet fuel gas. ASR = 0.20 Ω cm^2. Current density = 0.5 A/cm^2. Heat loss = 1% of input electricity. AC-DC converter efficiency = 97%.
Compressor/turbine	$\eta_{isentropic,\ compressor}$ = 88%, $\eta_{isentropic,\ turbine}$ = 90%
Ejector	$\eta \leq 25\%$ [d]
Methane reactors	Chemical equilibrium at reactor outlet temperature and pressure. Reactor outlet temperature of boiling water reactor: 280°C[e]. Reactor pressure: 20 bar. The gas module M for the gas entering the boiling water reactor is set to 3 (eq. (5))
Heat exchangers	ΔT_{min} = 30°C (gas-gas), ΔT_{min} = 10°C (gas-liq or gas - condens. gas), ΔT_{min} = 5°C (gas - boiling water)
Humidifier/condenser	ΔT_{min} = 5°C

[a] The sulfur content is neglected. The sulfur content is usually 0.01-0.02 wt% (dry), but can reach 0.1 wt% for brown wood pellets [24].

[b] The methane content will be lower than calculated by chemical equilibrium because the very high partial oxidation temperature (exceeding 1300°C) will convert all the methane. The methane formation reactions that occur in the following char reactor are very slow, so the methane content will not reach equilibrium.

[c] The inlet temperature on the fuel side is dictated by the upstream adiabatic methanator. The inlet temperature on the oxygen side is then set equal to this value.

[d] The ejector efficiency is 25% in the gasifier system, but only 2% is enough for the ejector in the SOEC system due to the high motive steam flow. The efficiency is defined as: $\eta_{EJECTOR} = \frac{\dot{V}_2 p_2 \ln(p_3/p_2)}{\dot{V}_1(p_1 - p_3)}$, where $\dot{V}$ is the volumetric flow rate, p is the pressure. The numbers 1 to 3 refer to: motive flow (1), recycled flow (2) and discharge flow (3) [4].

[e] The methanation catalysts from Haldor Topsøe can operate in a temperature span of 190°C to above 700°C [25,26].

3. Results and discussion

The results from the thermodynamic modelling of the SNG plant are summarized in Table 2 and Table 3 showing the energy inputs and outputs as well as the energy efficiencies and relevant energy ratios. Fig. 4 shows detailed results on the plant flowsheet, and in Table 4, the gas compositions are given for relevant mass flows.

The total efficiency of the plant is calculated to be 84%, which is significantly higher than the efficiency of a state-of-the-art plant with steam electrolysis (70%)[2]. A main reason for the higher efficiency is the internal methanation in the SOEC. It can be calculated from Table 4 that 47% of the produced methane

[2] The efficiency calculated in a study by Gassner et al. [9] is 69.6% for directly heated gasification and 73.1% for indirectly heated gasification (SNG_{max}, table 5 in [9]). This is however based on as received wood LHV (50 wt% water). If converted to dry wood basis to make the numbers comparable with data given in this paper, the numbers become 65.8% and 69.2% respectively.

is formed in the SOEC, 16% is formed before the SOEC in the adiabatic methanator, and the remaining 37% in the low-temperature methanator downstream the SOEC. In the case of steam electrolysis referred to in Table 3, 97% of the methane is formed in the low-temperature methanator and the remaining 3% is formed in the gasifier. It should be noted that other gasifier types could have a much higher internal methane production, but then tar removal will often also be an issue. The difference in methane formation in the LT methanator also impacts the efficiency of the LT methanator (92% with the electrocatalytic system vs. 82% with the steam electrolysis system) defined as $\frac{\dot{m}_{out} \cdot LHV_{out}}{\dot{m}_{in} \cdot LHV_{in}}$, where $\dot{m}$ is the mass flow rate and LHV is the lower heating value.

Pressurized operation of the stack is another main reason for the higher total efficiency. This can be seen by comparing the efficiency when auxiliary components are disregarded. By relating the two main energy inputs of biomass and electricity for the SOEC with the SNG output, the difference between the two plants is only 7%-points (82% vs. 75%, Table 3), while the difference was 14%-points for the total efficiency (84% vs. 70%). This shows that when operating pressurized it is possible to have a net production of electricity from the auxiliary components, while the auxiliary components will have a net electricity consumption when operating at atmospheric pressure. This is mainly due to pressurization of syngas to the LT methanator pressure in the case of operation at atmospheric pressure, and then turbine expansion of the excess oxygen produced by the pressurized SOEC in the case of pressurized operation. It should be noted that expansion of excess oxygen would be less attractive for pressurized steam electrolysis[3]. When comparing the present case with steam electrolysis, there are some minor differences in design and modelling approach that also affects the efficiencies. For example, the gasifier efficiency is 95% in this study and 93% in the other, and the modelling approach of the SOEC is less detailed in [8]. The gasifier efficiency, or cold gas efficiency, is defined as: $\frac{\dot{m}_{out} \cdot LHV_{out}}{\dot{m}_{in} \cdot LHV_{in}}$ (LHV on dry basis).

The SOEC efficiency is defined as the increase in heating value flow divided by the electricity input: $\frac{\dot{m}_{fuel,out} \cdot LHV_{fuel,out} - \dot{m}_{fuel,in} \cdot LHV_{fuel,in}}{Electricity}$.

A final thing to mention in the comparison with the state-of-the-art plant based on steam electrolysis is that the main difference in energy input is for electricity and not biomass. Table 3 shows that for every 100 MJ of SNG produced, 57-61 MJ of biomass is needed, while the electricity consumption varies from 62 to 84 MJ. This is because that both systems convert 98-99% of all the carbon in the biomass to CH_4, meaning that the biomass input is set by the carbon needed to produce the CH_4. Improvements in efficiency is therefore seen in the electricity consumption, which is reduced from 84 MJ to 62 MJ per 100 MJ of produced SNG.

Table 2

Energy inputs and outputs

Biomass input [MWth] (dry basis)	100.0
Electricity consumption: [MWe]	
Electrolysis	113.7
Oxygen/steam turbine	-6.2
Other components (compressors, blowers, pumps)	0.2
Net electricity consumption	107.7
SNG production [MWth]	174.2

[3] This is because that steam electrolysis is endothermic, meaning that it is highly beneficial to use the oxygen and hydrogen outputs to preheat the steam input, thereby reducing the electricity input to the electrolyser. Furthermore, the oxygen expansion would require a turbine made for pure oxygen.

Table 3

Energy efficiencies and energy ratios

Energy efficiencies [%]:	Electrocatalysis	Steam electrolysis[a]
Biomass to syngas (cold gas efficiency)	95	93
SOEC efficiency	91	92
LT methanator efficiency	92	82
Biomass + electricity to SNG (total efficiency)	84	70
Biomass + SOEC electricity to SNG	82	75
Energy ratios [%]:		
Biomass input to SNG output	174	165
Electricity input to SNG output	162	119
Biomass input per SNG output	57	61
Electricity input per SNG output	62	84

[a] Steam electrolysis refers to the state-of-the-art system, see Fig. 1. The numbers are from [8]. The study considers biomasses with different ash content. The results shown are for low ash biomass (1% ash) in order to make the comparison fair. It should be noted that the gasifier and SOEC are at atmospheric pressure.

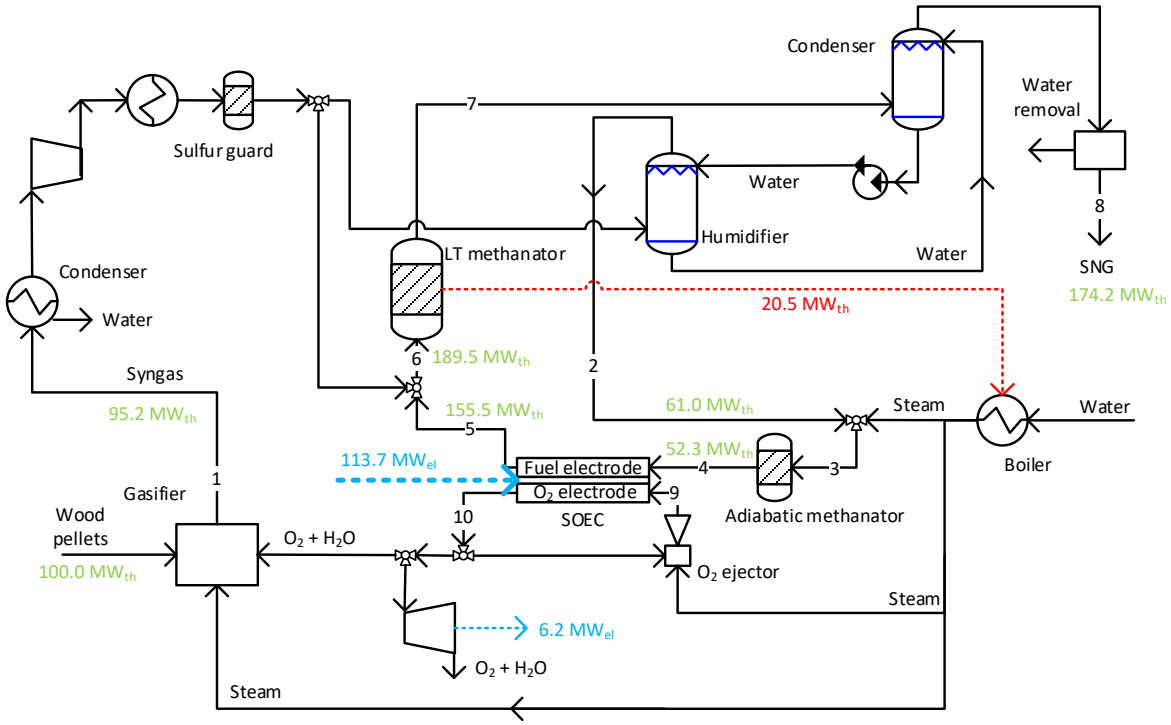

Fig. 4. Flowsheet of the proposed design integrating pressurized SOEC and biomass gasification for SNG production. The figure includes electricity consumptions and productions (blue), as well as chemical energy flows (LHV dry, green) and major heat flows (red). Stream numbers refer to Table 4 with gas compositions. A more detailed flowsheet can be found in appendix. Note that the boiler shown in this figure represents two boilers in the detailed flowsheet in appendix.

Table 4

Stream compositions (stream numbers refer to Fig. 4)

	Gasifier outlet	Humidifier outlet	Adiabatic methanator inlet	SOEC fuel inlet	SOEC fuel outlet	LT methanator inlet	LT methanator outlet	SNG	SOEC O_2 inlet	SOEC O_2 outlet
Stream number	1	2	3	4	5	6	7	8	9	10
Mass flow[kg/s]	9.97	7.83	11.26	11.26	3.32	6.16	6.16	3.53	26.81	34.75
Mole flow [kmole/s]	0.570	0.445	0.635	0.567	0.365	0.529	0.368	0.222	1.455	1.371
Mole%										
H_2	41.8	34.3	24.0	16.0	52.1	52.1	1.4	2.4	-	-
CO	23.4	19.2	13.4	1.8	0.8	9.6	~0[b]	~0[c]	-	-
CO_2	14.7	12.1	8.5	16.7	0.2	5.9	0.4	0.6	-	-
H_2O	20.1	34.5	54.1	59.5	9.8	6.8	39.6	-	58.1	47.6
CH_4	~0[a]	~0	~0	6.0	37.1	25.6	58.5	96.9	-	-
N_2	~0	~0	~0	~0	~0	~0	~0	0.1	-	-
O_2	-	-	-	-	-	-	-	-	41.9	52.4

[a] see footnote b at Table 1 about the low methane content. [b] 2 ppm CO. [c] 4 ppm CO.

Table 5 shows calculated SOEC parameters. It can be seen that the oxygen utilization factor is very high (92.5%), probably too high for future commercial SOEC stacks. The oxygen utilization factor is defined as the transferred oxygen in the SOEC divided by the total oxygen input from the fuel gas: $\frac{2\dot{n}_{O_2,transferred}}{2\dot{n}_{CO_2}+\dot{n}_{CO}+\dot{n}_{H_2O}}$. The main issue with a high stack utilization factor is that the flow distribution to the individual cells must be highly uniform, otherwise the fuel gas at some cells will run out of oxygen, which will cause irreversible damage to the cells. There are many ways of reducing the oxygen utilization factor for the stack, but a simple way is to have stacks in series. If two stacks are in series and have the same oxygen transfer (same current). Then they would be able to achieve an overall oxygen utilization factor of 92.5% by having an utilization factor of 46.25% ($\frac{92.5\%}{2}$) in the first stack, and then 86.0% ($\frac{46.25\%}{100\%-46.25\%}$) in the second stack. The main concern of having stacks in series is pressure drop, but this is not a big issue for pressurized stacks as the pressure drop is approximately inverse proportional to the operation pressure [27]. Another option is to have a recycle flow on the fuel side by an ejector. This would have the added benefit of increasing the temperature before the stack, which lowers the stack thermal stresses as well as the average stack ASR.

Table 5

Calculated SOEC parameters

Oxygen utilization factor	92.5%
H/C molar ratio	7.14
Cell voltage [V]	1.151
$E_{Nernst,\ average}$ [V]	1.051
$E_{Nernst,\ inlet,\ co\text{-}flow}$[a] [V]	1.021
$E_{Nernst,\ outlet,\ co\text{-}flow}$ [V]	1.125
$E_{Nernst,\ inlet,\ counter\text{-}flow}$[a] [V]	1.025
$E_{Nernst,\ outlet,\ counter\text{-}flow}$ [V]	1.121
Total active cell area [m^2]	19 160

[a] Note that the inlet Nernst potentials are close to the average Nernst potential as the average Nernst potential is calculated at constant temperature (the outlet temperature).

The H/C ratio of the fuel gas in the SOEC is calculated as the operating point where the steam supply matches the steam demand, as illustrated in Fig. 5. The steam supply depends on the heat available at the LT methanator: at higher H/C ratio, the mass flow of syngas bypassing the SOEC increases. This fosters a higher methane production in the LT methanator, which leads to a larger steam production. As previously mentioned, the steam demand depends on the gasifier, the fuel gas and the steam sweep in the SOEC. Thus, the H/C ratio in the SOEC is 7.14, which is higher than the minimum H/C ratio predicted by thermodynamics (6.05 @ 700°C and 20 bar [6]). The higher total steam demand at low H/C ratio is dictated by the higher cooling demand of the SOEC, caused by the more exothermic operation of the SOEC. At low H/C ratio, the lower H_2O content leads to a lower extent of the endothermic steam electrolysis reaction in the SOEC. The exothermic methane reactions will therefore dominate and require more cooling of the SOEC. Fig. 5 also shows that the fuel gas steam demand only increases slightly with H/C ratio, which is because most of the extra steam needed by the fuel gas to reach the set H/C ratio is supplied by the humidifier and not through the steam generator (Fig. 6). The steam demand for the gasifier increases with H/C ratio as the steam content of the O_2/H_2O mixture used by the gasifier decreases.

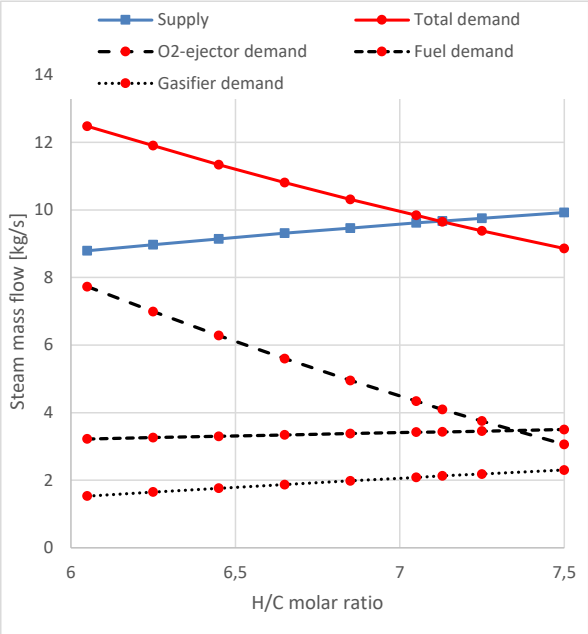

Fig. 5. Mass flow of steam vs. H/C ratio. The calculated H/C ratio for the system is found at the intersection between supply and demand curves (H/C = 7.14).

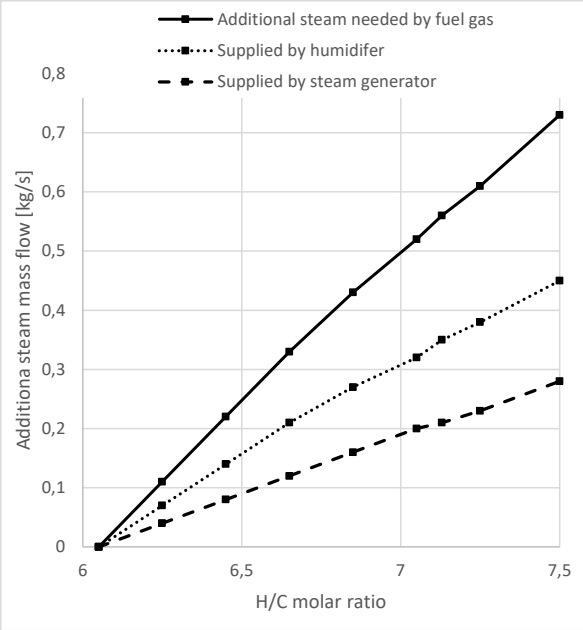

Fig. 6. Additional steam mass flow vs. H/C ratio. The figure shows how the demand for additional steam by the fuel gas is met by the humidifier and the steam generator.

3.1 Reducing electricity consumption by introducing an external heat supply for the steam generator

It would be beneficial for the system if the steam sweep on the oxygen electrode of the SOEC could be increased as this would lower the O_2%, which would ease oxygen handling around the SOEC including the H_2O/O_2-turbine, but also lower the Nernst potential and thereby reduce the electricity consumption of the SOEC. Furthermore, the electricity production of the H_2O/O_2-turbine would be increased due to the increased steam mass flow. Increasing the steam sweep will however require more heat, which is not available in the system. If an external waste heat supply at approx. 225°C could be identified, it would be possible to raise saturated steam at 22 bar for the ejector. As shown on Fig. 5, the steam demand increased when decreasing the H/C ratio. It is therefore possible to accommodate an external heat supply if the H/C ratio is reduced. Fig. 7 shows how much external heat that could be added to the system, and what the reduction in the net power consumption would be. The main reason for the reduction in the net power consumption is seen to be the increase in power production of the H_2O/O_2-turbine, while the reduction in SOEC power is almost insignificant. The relation between the net power reduction and heat addition can be shown as an efficiency of a heat engine. The figure shows that this efficiency would be 35-37%, which is high when considering that the external heat is needed at or below 225°C. For comparison, the Carnot efficiency is 41% when the heat source temperature is 225°C (heatsink temperature at 20°C).

It should be noted that the risk of carbon deposition inside the fuel electrode increases with decreasing H/C ratio. Furthermore, it is expected that the H/C ratio at the triple phase boundary is lower than the bulk gas H/C ratio because of the high diffusion coefficient for H_2 compared with the coefficients for H_2O, CO, CO_2 and CH_4. Consequently, the lower limit for the H/C ratio is determined by several parameters such as current density, electrode porosity/tortuosity, thickness, catalytic activity and fuel flow uniformity in the gas channels. It is beyond the scope of this paper to quantify the lower limit for the H/C ratio, but improved electrode configurations not having Ni at the triple phase boundaries (but still having Ni in the support layer or current collector layer) could help reaching stable operation with H/C ratios relatively close to the carbon formation ratio limit for the bulk-gas [28].

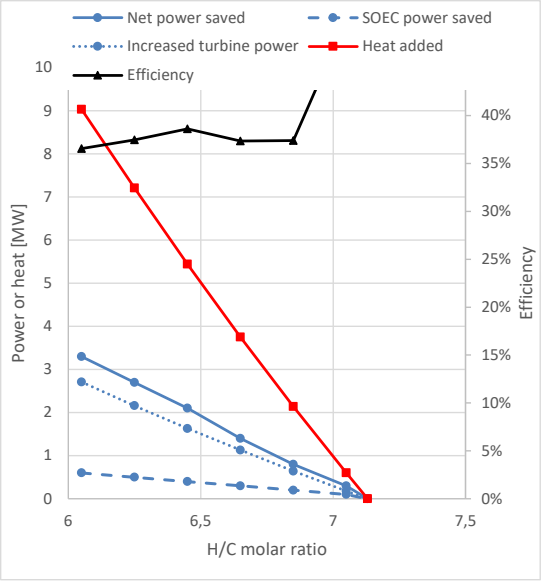

Fig. 7. Net power saved when introducing external heat to the steam generator. The H/C ratio is reduced with heat addition.

3.2 Adding a recuperative heat exchanger to increase H/C ratio and SOEC inlet temperature

If the H/C ratio needs to be unchanged or even higher than 7.14, a recuperative heat exchanger can be added to the fuel side of the SOEC as illustrated on Fig. 8. This method can also increase the fuel inlet temperature to the SOEC from 614°C to 700°C.

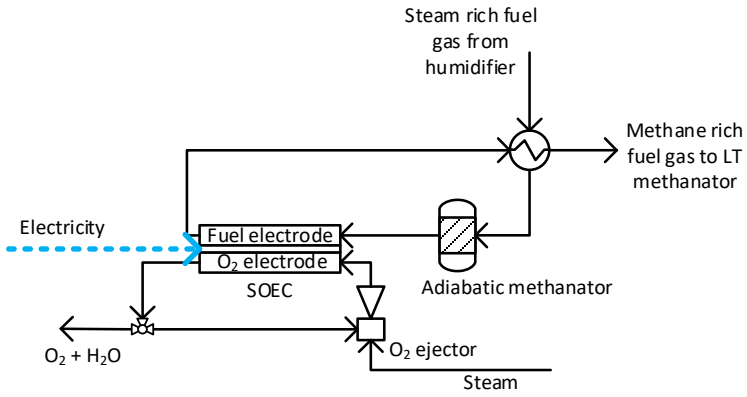

Fig. 8. Implementation of recuperator on the fuel side of the SOEC to enable higher H/C ratio and inlet temperature.

If a minimum temperature difference of 50°C is applied to the recuperator, then the H/C ratio cannot be lower than 7.04 if the fuel inlet temperature to the SOEC is restricted to the operating temperature of the SOEC (700°C). At this operating point, the system would be able to convert 14.3 MW of external heat supply into a net power reduction of 5.1 MW, corresponding to a heat to power efficiency of 36% (Table 6). If the H/C ratio needs to be 7.5, the external heat input would drop to 10.3 MW and the fuel inlet temperature to the SOEC would drop to 689°C. However, the heat to power efficiency would be almost constant (35%, see Table 6).

As mentioned, operating at an H/C ratio, which is significantly higher than the minimum H/C ratio needed to avoid carbon deposition in the bulk gas could be attractive, mainly because the local H/C ratio at the triple phase boundary is expected to be lower than the bulk gas H/C ratio.

The recuperator can also be used to increase the H/C ratio without having any external heat input. This is the final case investigated in Table 6. By comparing to the base case, it only costs 0.1 MW of net power to go from an H/C ratio of 7.14 to 7.5. On top of this comes the capital cost of the recuperator, but this is not high as only 1 MW of heat is transferred, and the minimum temperature difference in the recuperator is very high for this case (294°C).

Table 6
Comparing the base case with cases with and without recuperator for two different H/C ratios.

	Base case	Without recuperator		With recuperator		
H/C ratio	7.14	7.04	7.50	7.04	7.50	7.50
$T_{\text{fuel inlet SOEC}}$ [°C]	614	617	605	700	689	623
$\Delta T_{\text{min, recuperator}}$	-	-	-	50	50	294
$\dot{Q}_{\text{recuperator}}$ [MW]	-	-	-	5.4	5.2	1.0
$\%O_{2,\text{ outlet SOEC}}$	52	51	59	32	36	52
Heat added [MW]	-	0.6	-2.6	14.3	10.3	-
Net Power saved [MW]	-	0.3	-1	5.1	3.6	-0.1
Efficiency[a] [%]	-	-	-	36	35	-
Carnot efficiency ratio[b] [%]	-	-	-	87	85	-

[a] defined as "heat added" to "net power saved". [b] defined as the efficiency of a Carnot cycle using the same heat source temperature of 225 C ($1-T_L/T_H$ = 1-293/498 = 41%) relative to the actual efficiency given in the table.

3.3 Replacing wood pellets with less expensive wood chips

Converting the system from wood pellets to a cheaper biomass such as wood chips could be economically attractive. Currently, wood chips are traded mainly for pulp and paper, but also for bioenergy. The price for wood chips for pulp and paper is similar to the wood pellet price in terms of cost per unit of energy according to FOEX Indexes Ltd in Finland [29]. The pellet price is currently at 29.2 €/MWh (PIX Pellet Nordic), but the price in Finland for "forest biomass" which is mainly wood chips for energy (PIX Forest Biomass Finland) is at 18.35 €/MWh [29]. Replacing wood pellets with wood chips can therefore result in a significant cost reduction.

The system does not currently have enough waste heat to cover drying of input biomass in case of using wood chips instead of wood pellets. The moisture content of wood chips vary greatly, but can be 50 wt% or more. It is assumed that the water content of wood chips is 50 wt%, while it was assumed to be 7 wt% for wood pellets. An external heat supply was discussed in section 3.1, and this could of course be used for biomass drying. However, it would be relevant to determine the reduction in system performance when forcing the system to accommodate the heat consumption of biomass drying. The main internal heat consumption is for steam generation to cover the steam sweep on the oxygen electrode of the SOEC. A lot of heat could therefore be made available for biomass drying by reducing the steam sweep. When reducing the steam sweep, the oxygen fraction will increase beyond 52 vol% (to 75 vol%), complicating the oxygen/steam handling - especially regarding the oxygen turbine. Because the steam sweep is set by the cooling demand of the SOEC, it is necessary to find another way of cooling the SOEC. The simplest solution is to cool with the fuel flow. This can be achieved by using an ejector on the fuel side, and then cooling the fuel gas prior to the ejector. Furthermore, to avoid an extremely high recycle ratio on the fuel ejector and to reduce the exothermic behavior of the SOEC, a second adiabatic reactor is placed after the fuel cooling, just before the fuel ejector (Fig. 9). By reducing the steam consumption for the steam sweep and instead cooling on the fuel side, a significant waste heat flow is made available for biomass drying (15.8 MWth, Fig. 9). The needed heat flow for drying is found by setting the moisture content of dry wood chips to 2 wt%. For simplicity, it is assumed that the dry biomass composition and heating value is unchanged, but in reality, the ash content would be higher for wood chips than for wood pellets. The impact of a higher ash content is however insignificant.

Fig. 9 shows the flowsheet of the system based on wood chips, and Table 7 gives the main gas compositions.

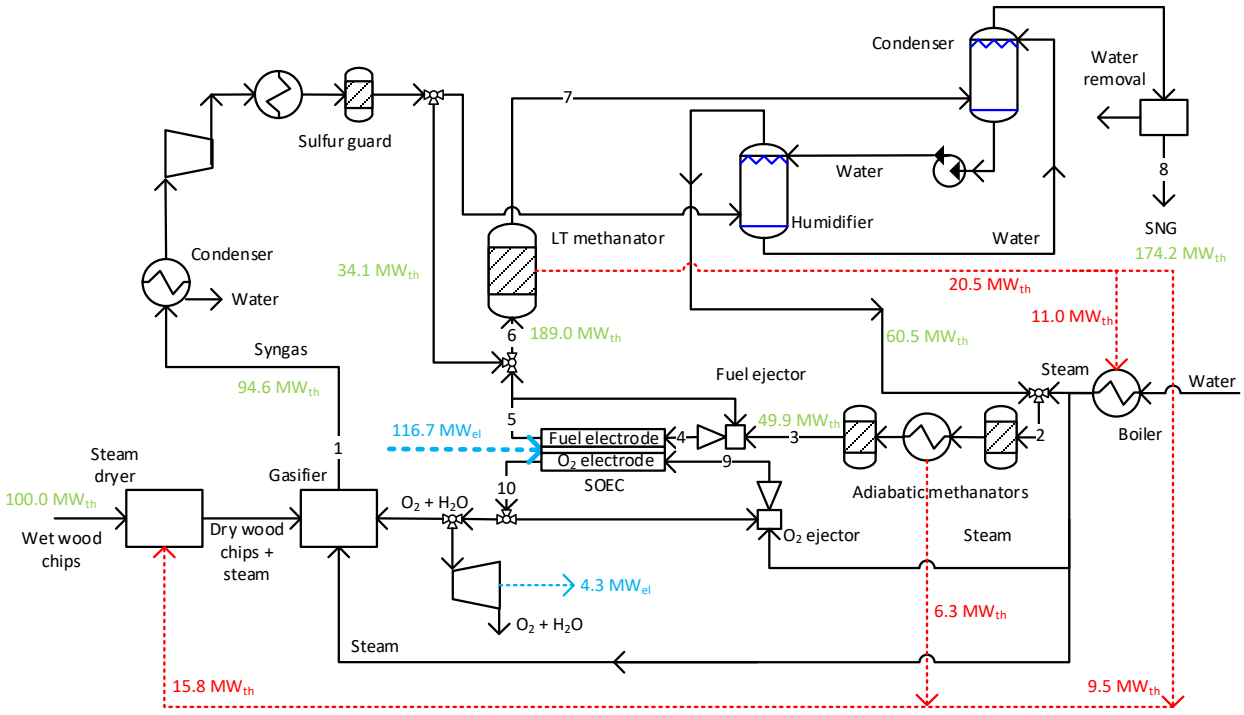

Fig. 9. Flowsheet of the design using wood chips instead of wood pellets. The figure includes electricity consumptions and productions (blue), as well as chemical energy flows (green, LHV dry) and major heat flows (red). Stream numbers refer to Table 7 with gas compositions. A more detailed flowsheet can be found in appendix. Note that the boiler shown in this figure represents two boilers in the detailed flowsheet in appendix.

Table 7

Stream compositions (stream numbers refer to Fig. 9)

	Gasifier outlet	Adiabatic methanator inlet	Fuel ejector inlet	SOEC fuel inlet	SOEC fuel outlet	LT methanator inlet	LT methanator outlet	SNG	SOEC O_2 inlet	SOEC O_2 outlet
Stream number	1	2	3	4	5	6	7	8	9	10
Mass flow [kg/s]	13.84	11.18	11.18	19.79	11.92	6.43	6.43	3.53	18.19	26.06
Mole flow [kmole/s]	0.788	0.634	0.534	1.472	1.311	0.544	0.383	0.222	0.669	0.916
Mole%										
H_2	35.8	28.5	7.3	36.0	52.1	53.5	1.5	2.5	-	-
CO	11.8	9.4	0.3	0.6	0.8	6.7	~0[a]	~0[b]	-	-
CO_2	15.7	12.5	16.3	6.0	0.2	8.4	0.4	0.6	-	-
H_2O	36.6	49.6	66.7	30.3	9.8	6.6	41.9	~0	34.6	25.3
CH_4	~0	~0	9.3	27.1	37.1	24.8	56.2	96.8	-	-
N_2	~0	~0	~0	~0	~0	~0	~0	0.1	-	-
O_2	-	-	-	-	-	-	-	-	65.4	74.7

[a] 2 ppm CO. [b] 4 ppm CO.

The figure shows that the main heat supply for biomass steam drying comes from the LT methanator, mainly because the steam consumption for the steam sweep is reduced. However, the steam consumptions for fuel injection and gasifier are also reduced, due to the high steam input to the gasifier from the steam dryer, also resulting in a higher hydrogen content of the gasifier syngas. The higher hydrogen content reduces the steam consumption of the fuel gas to reach an H/C ratio of 7.14. The H/C ratio is kept constant compared with the base system on wood pellets by adjusting the fuel cooling between the two adiabatic methanators. The main energy flows are shown on Fig. 9, but also summarized and compared with the base case in Table 8. It can be seen from the table that the net electricity consumption is increased when using wood chips instead of wood pellets. This is due to 1) an increase in the SOEC power because of the added fuel ejector increasing the inlet Nernst voltage, and 2) a lower oxygen turbine power output because of the reduced steam sweep on the oxygen electrode. The higher net electricity consumption also results in slightly lower system efficiencies as seen in Table 9. The increase in electricity consumption could be converted to a coefficient of performance (COP), as electricity is indirectly used to provide heat for drying. The COP can be calculated to be 2.8 (15.8 MWth / 5.7 MWe).

The increase in inlet Nernst voltage by the added fuel ejector can be seen from Table 10, but the table also shows that the fuel ejector significantly reduces the oxygen utilization factor. The fuel flow recycle by the ejector is calculated by setting the inlet fuel gas temperature to the SOEC to 630°C. This is slightly higher than the inlet temperature in the base system, which was calculated by the adiabatic methanator to be 614°C. The added fuel ejector therefore improves the SOEC operating conditions, but at the cost of a higher SOEC power consumption. The higher net electricity consumption of the system on wood chips results in a higher cost for electricity compared to the base case system on wood pellets. Based on the current price difference between wood chips and wood pellets it can be calculated that this extra electricity cost is compensated by the reduced biomass cost[4].

Table 8

Energy inputs and outputs compared with the base case system on wood pellets

	Wood chips	Wood pellets
Biomass input [MWth]	100.0	100.0
Electricity consumption: [MWe]		
Electrolysis	116.7	113.7
Oxygen/steam turbine	-4.3	-6.2
Other components (compressors, blowers, pumps)	1.0	0.2
Net electricity consumption	113.4	107.7
SNG production [MWth]	174.2	174.2

[4] If the biomass prices stated above are used (29.2 €/MWh for pellets and 18.35 €/MWh for chips [29]) the electricity price needs to be 190 €/MWh to balance out the reduction in biomass cost. The average current electricity price in Denmark and Europe for large industries (70-150 GWh) is a bit below 80 €/MWh including taxes, distribution etc. [30]. However, electrolysis for fuel production would only be adopted with electricity prices similar to biomass prices (~30 €/MWh).

Table 9

Energy efficiencies compared with the base case system on wood pellets

Energy efficiencies [%]:	Wood chips	Wood pellets
Biomass to syngas (cold gas efficiency)	95	95
SOEC efficiency	90	91
LT methanator efficiency	92	92
Biomass + electricity to SNG (total efficiency)	82	84
Biomass + SOEC electricity to SNG	80	82

Table 10

Calculated SOEC parameters compared with the base case system on wood pellets

	Wood chips	Wood pellets
Oxygen utilization factor	77.3%	92.5%
H/C molar ratio	7.14	7.14
Cell voltage [V]	1.193	1.151
$E_{Nernst,\ average}$ [V]	1.093	1.051
$E_{Nernst,\ inlet,\ co\text{-}flow}$ [V]	1.077	1.021
$E_{Nernst,\ outlet,\ co\text{-}flow}$ [V]	1.133	1.125
$E_{Nernst,\ inlet,\ counter\text{-}flow}$ [V]	1.079	1.025
$E_{Nernst,\ outlet,\ counter\text{-}flow}$ [V]	1.130	1.121
Total active cell area [m^2]	18 990	19 160

4. Conclusion

Integrated electrolysis and gasification based systems for biofuel production can be attractive systems because they can ensure almost 100% carbon efficiency and can act as a flexible demand for renewable electricity producers. This paper has shown by thermodynamic modelling that highly energy efficient production of synthetic natural gas can be achieved when feeding biomass syngas to pressurized solid oxide electrolysis cells mainly because of methanation reactions occurring inside the SOEC. The system achieved a biomass + electricity to SNG energy efficiency of 84%, which can be compared with an efficiency of 70% for a state of the art system using steam electrolysis. Saturated steam was used to sweep the oxygen electrode and to cool the SOEC. This enabled the system to convert external low temperature heat to saturated steam, which could reduce the net power consumption with a very high heat-to-electricity efficiency of 35-37%, which can be compared with a Carnot efficiency of 41%. The system was designed without recuperative heat exchangers for the SOEC, but could achieve isothermal conditions on the fuel side of the SOEC by integration of a small recuperative heat exchanger.
If the gasifier feedstock was changed from wood pellets to wood chips with the added integration of steam drying, the overall efficiency was reduced from 84% to 82% due to a higher net electricity consumption. The extra electricity cost would however be compensated by the reduced biomass feedstock cost, making the switch to wood chips economically attractive.

Declarations of interest

None

References

[1] Jensen SH, Langnickel H, Hintzen N, Chen M, Hauch A, Butera G, et al. Pressurized reversible operation of a 30-cell solid oxide cell stack using carbonaceous gases. European Fuel Cell Technology & Applications Conference - Piero Lunghi Conference, ENEA; 2017.

[2] Bierschenk DM, Wilson JR, Barnett SA. High efficiency electrical energy storage using a methane–oxygen solid oxide cell. Energy Environ Sci 2011;4:944–51.

[3] Momma A, Takano K, Tanaka Y, Kato T, Yamamoto A. Experimental Investigation of the Effect of Operating Pressure on the Performance of SOFC and SOEC. ECS Trans 2013;57:699–708.

[4] Wendel CH, Kazempoor P, Braun RJ. Novel electrical energy storage system based on reversible solid oxide cells: System design and operating conditions. J Power Sources 2015;276:133–44.

[5] Jensen SH, Graves C, Mogensen M, Wendel C, Braun R, Hughes G, et al. Large-scale electricity storage utilizing reversible solid oxide cells combined with underground storage of CO2 and CH4. Energy Environ Sci 2015;8:2471–9.

[6] Butera G, Jensen SH, Clausen LR. A novel system for large-scale storage of electricity as synthetic natural gas using reversible pressurized solid oxide cells. Energy 2019;166:738–54.

[7] Clausen LR. Maximizing biofuel production in a thermochemical biorefinery by adding electrolytic hydrogen and by integrating torrefaction with entrained flow gasification. Energy 2015;85:94–104.

[8] Clausen LR. Energy efficient thermochemical conversion of very wet biomass to biofuels by integration of steam drying, steam electrolysis and gasification. Energy 2017;125.

[9] Gassner M, Maréchal F. Thermo-economic optimisation of the integration of electrolysis in synthetic natural gas production from wood. Energy 2008;33:189–98.

[10] Pozzo M, Lanzini A, Santarelli M. Enhanced biomass-to-liquid (BTL) conversion process through high temperature co-electrolysis in a solid oxide electrolysis cell (SOEC). Fuel 2015;145:39–49.

[11] Martínez I, Romano MC. Flexible sorption enhanced gasification (SEG) of biomass for the production of synthetic natural gas (SNG) and liquid biofuels: Process assessment of stand-alone and power-to-gas plant schemes for SNG production. Energy 2016;113:615–30.

[12] Barelli L, Bidini G, Cinti G. Steam as sweep gas in SOE oxygen electrode. J Energy Storage 2018;20:190–5.

[13] Abdoulmoumine N, Adhikari S, Kulkarni A, Chattanathan S. A review on biomass gasification syngas cleanup. Appl Energy 2015;155:294–307.

[14] Syngas purification | Haldor Topsoe. https://www.topsoe.com/processes/syngas/syngas-purification (accessed January 30, 2019).

[15] Elmegaard B, Houbak N. DNA - a general energy system simulation tool. SIMS 2005, 46th conference on simulation and modeling, Trondheim, Norway: 2005, p. 43–52.

[16] Tech. Univ. Denmark - Mech. Eng. Dep. Homepage of the thermodynamic simulation tool DNA. http://orbit.dtu.dk/query?record=231251 (accessed January 30, 2019).

[17] Ahrenfeldt J, Henriksen U, Jensen TK, Gøbel B, Wiese L, Kather A, et al. Validation of a continuous combined heat and power (CHP) operation of a two-stage biomass gasifier. Energy and Fuels 2006;20:2672–80.

[18] Henriksen U, Ahrenfeldt J, Jensen TK, Gøbel B, Bentzen JD, Hindsgaul C, et al. The design, construction and operation of a 75 kW two-stage gasifier. Energy 2006;31:1542–53.

[19] Gadsbøll RØ, Clausen LR, Thomsen TP, Ahrenfeldt J, Henriksen UB. Flexible TwoStage biomass gasifier designs for polygeneration operation. Energy 2019;166:939–50.

[20] The National Energy Technology Laboratory (NETL). Lurgi Dry-Ash Gasifier. https://www.netl.doe.gov/research/coal/energy-systems/gasification/gasifipedia/lurgi (accessed November 30, 2018).

[21] He C, Feng X, Chu KH. Process modeling and thermodynamic analysis of Lurgi fixed-bed coal

gasifier in an SNG plant. Appl Energy 2013;111:742–57.
[22] Lurgi FBDB™ - Fixed Bed Dry Bottom Gasification | Air Liquide. https://www.engineering-airliquide.com/lurgi-fbdb-fixed-bed-dry-bottom-gasification (accessed January 30, 2019).
[23] Skafte TL, Blennow P, Hjelm J, Graves C. Carbon deposition and sulfur poisoning during CO 2 electrolysis in nickel-based solid oxide cell electrodes. J Power Sources 2018;373:54–60.
[24] Energy research Centre of the Netherlands. Phyllis2, database for biomass and waste. https://www.ecn.nl/phyllis2 (accessed January 30, 2019).
[25] Haldor Topsoe. Mehtanation catalysts from Haldor Topsoe A/S. https://www.topsoe.com/products/pk-7r (accessed January 30, 2019).
[26] Halder Topsøe. From solid fuels to substitute natural gas (SNG) using TREMP 2009. https://docplayer.net/9077755-From-solid-fuels-to-substitute-natural-gas-sng-using-tremp.html (accessed January 30, 2019).
[27] Jensen SH, Sun X, Ebbesen SD, Chen M. Pressurized Operation of a Planar Solid Oxide Cell Stack. Fuel Cells 2016;16:205–18.
[28] Skafte TL, Sudireddy BR, Blennow P, Graves C. Carbon and Redox Tolerant Infiltrated Oxide Fuel-Electrodes for Solid Oxide Cells. ECS Trans 2016;72:201–14.
[29] Foex Indexes Ltd. Bioenergy and Wood Indices. http://www.foex.fi/biomass/ (accessed January 30, 2019).
[30] The Danish Energy Agency. Facts on electricity prices for business and industry (in Danish). https://ens.dk/ansvarsomraader/energi-klimapolitik/erhvervslivets-energiforhold/fakta-om-elpriser-erhverv-og (accessed January 30, 2019).

Appendix

Detailed flowsheet of the base case system using wood pellets

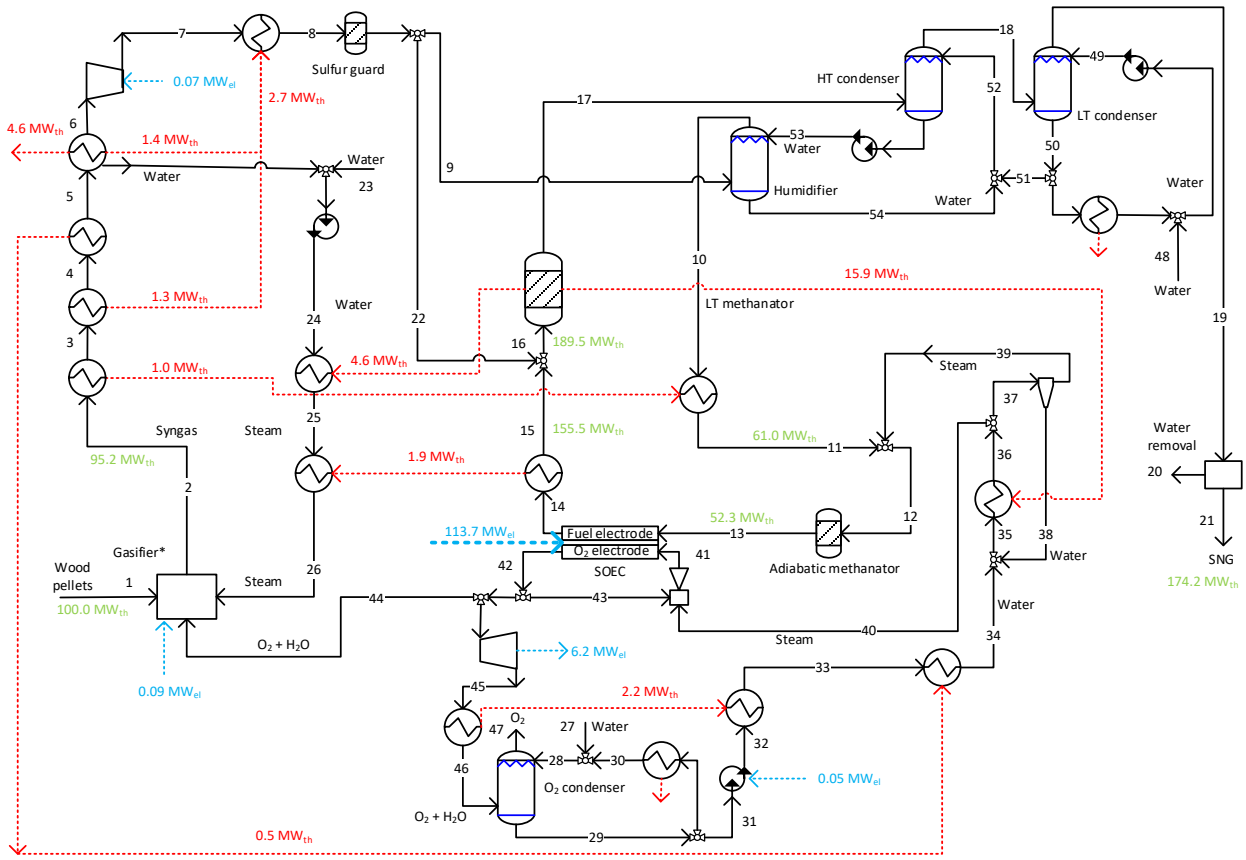

	t (C)	p (bar)	m (kg/s)
1	20	-	5.88
2	305	19.00	9.97
3	250	19.00	9.97
4	182	19.00	9.97
5	155	19.00	9.97
6	30	19.00	7.92
7	35	20.03	7.92
8	220	20.03	7.92
9	220	20.03	5.08
10	164	20.03	7.83
11	235	20.03	7.83

	t (C)	p (bar)	m (kg/s)
12	228	20.03	11.26
13	614	20.03	11.26
14	700	20.00	3.32
15	587	20.00	3.32
16	493	20.00	6.16
17	280	20.00	6.16
18	144	20.00	4.54
19	30	20.00	3.54
20	30	20.00	0.01
21	30	20.00	3.53
22	220	20.03	2.84

	t (C)	p (bar)	m (kg/s)
23	25	19.00	0.08
24	145	55.03	2.13
25	270	55.03	2.13
26	600	55.03	2.13
27	25	1.00	4.28
28	25	1.00	37.37
29	75	1.00	40.58
30	25	1.00	33.09
31	75	1.00	7.49
32	76	59.46	7.49
33	145	59.46	7.49

	t (C)	p (bar)	m (kg/s)
34	160	59.46	7.49
35	160	59.46	7.52
36	275	59.46	7.52
37	275	59.46	3.46
38	212	20.03	0.02
39	212	20.03	3.43
40	275	59.46	4.06
41	614	20.03	26.81
42	700	20.00	34.75
43	700	20.00	22.75
44	700	20.00	2.01

	t (C)	p (bar)	m (kg/s)
45	257	1.00	9.99
46	86	1.00	9.99
47	30	1.00	6.78
48	25	20.00	0.13
49	25	20.00	6.60
50	139	20.00	7.60
51	139	20.00	1.13
52	139	20.00	40.76
53	169	20.03	42.38
54	139	20.03	39.63

* the gasifier flowsheet can be seen on the next figure

Detailed flowsheet of the gasifier using wood pellets

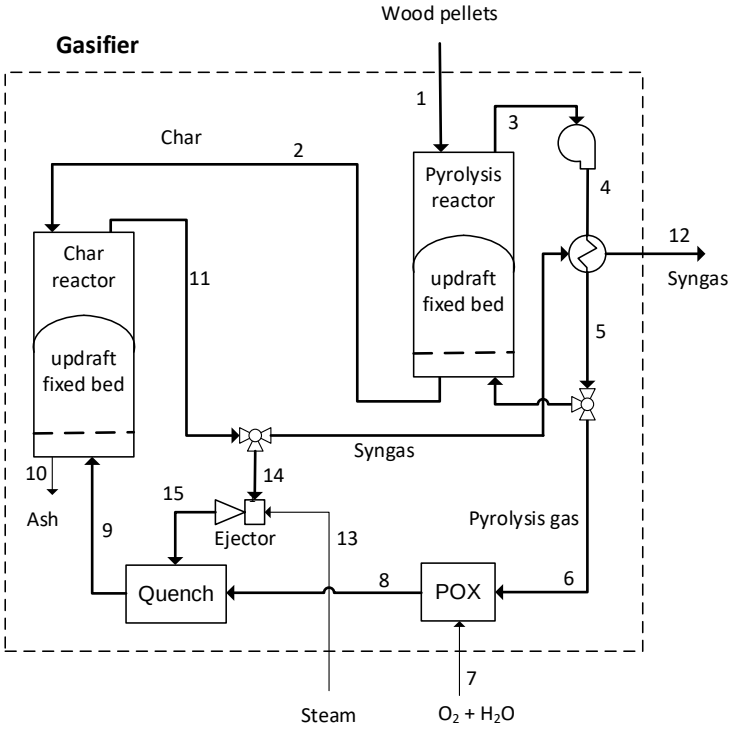

	t (C)	p (bar)	m (kg/s)
1	20	-	5.88
2	700	-	1.37
3	248	19.01	10.41
4	253	19.32	10.41
5	700	19.31	10.41
6	700	19.31	4.51
7	700	19.31	2.01
8	1626	19.31	6.53
9	950	19.31	26.77
10	940	-	0.06
11	750	19.01	28.11
12	305	19.00	9.97
13	600	55.03	2.13
14	750	19.01	18.14
15	731	19.31	20.27

Stream compositions (stream numbers refer to the figure above)

	Pyrolysis gas	Oxidizer (O_2 + H_2O)	Partially oxidized gas	Ejector outlet gas	Quench gas	Syngas
Stream number	6	7	8	15	9	12
Mass flow [kg/s]	4.51	2.01	6.53	20.27	26.8	9.97
Mole flow [kmole/s]	0.219	0.079	0.336	1.155	1.491	0.570
Mole%						
H_2	4.5	-	23.1	37.5	34.2	41.8
CO	33.8	-	24.0	21.0	21.7	23.4
CO_2	1.1	-	10.5	13.2	12.6	14.7
H_2O	42.6	47.6	42.4	28.3	31.5	20.1
CH_4	18.0	-	~0	~0	~0	~0
N_2	~0	-	~0	~0	~0	~0
O_2	-	52.4	-	-	-	-

[a] 2 ppm CO. [b] 4 ppm CO.

Detailed flowsheets of the system using wood chips

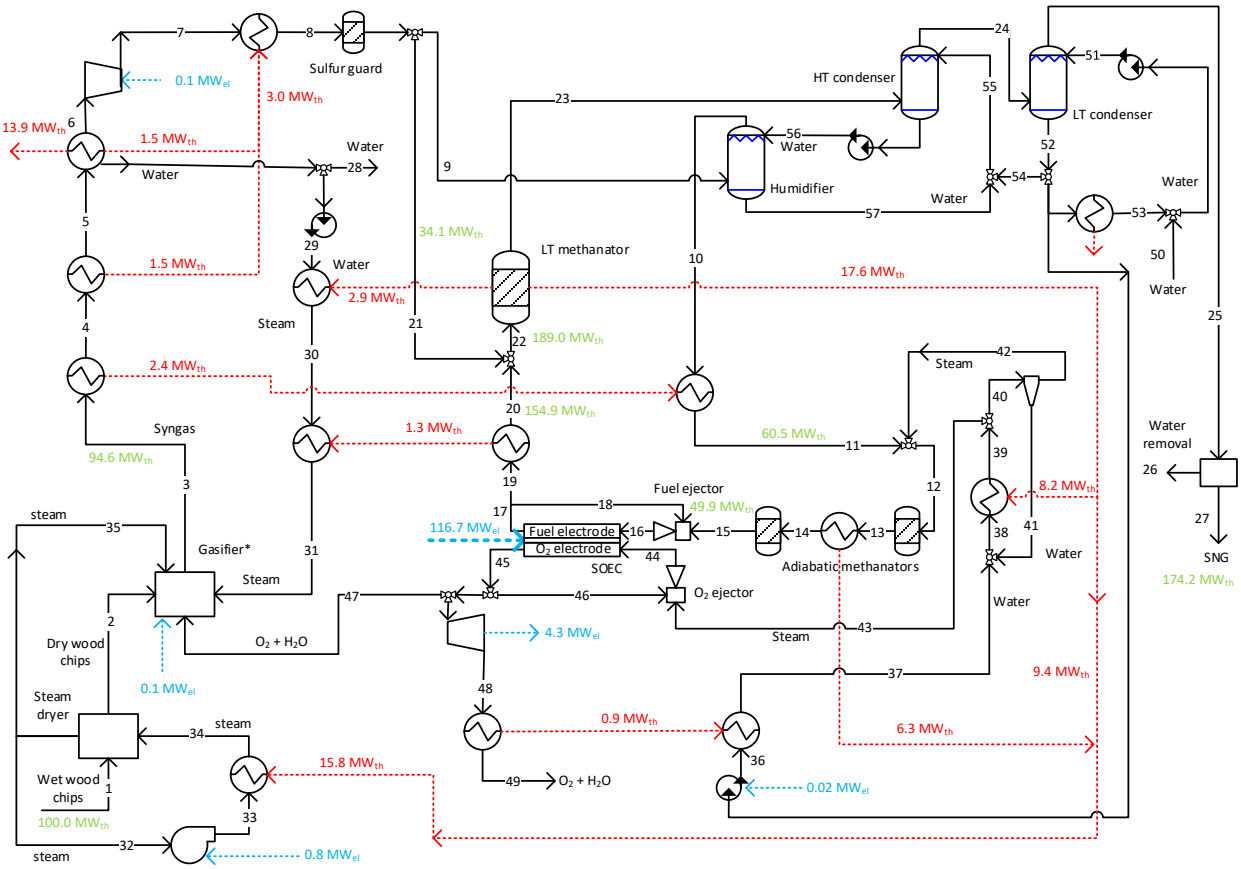

	t (C)	p (bar)	m (kg/s)
1	20	-	10.94
2	250	-	5.58
3	342	19.00	13.84
4	252	19.00	13.84
5	197	19.00	13.84
6	30	19.00	8.65
7	36	20.30	8.65
8	222	20.30	8.65
9	222	20.30	5.53
10	165	20.30	8.58
11	312	20.30	8.58

	t (C)	p (bar)	m (kg/s)
12	289	20.30	11.18
13	628	20.30	11.18
14	336	20.30	11.18
15	498	20.30	11.18
16	630	20.03	19.79
17	700	20.00	11.92
18	700	20.00	8.61
19	700	20.00	3.31
20	623	20.00	3.31
21	222	20.00	3.12
22	511	20.00	6.43

	t (C)	p (bar)	m (kg/s)
23	280	20.00	6.43
24	145	20.00	4.57
25	30	20.00	3.54
26	30	20.00	0.01
27	30	20.00	3.53
28	-	19.00	3.73
29	187	55.03	1.46
30	270	55.03	1.46
31	600	55.03	1.46
32	220	19.01	88.24
33	224	19.41	88.24

	t (C)	p (bar)	m (kg/s)
34	295	19.31	88.24
35	220	19.01	5.36
36	140	59.46	4.10
37	188	59.46	4.10
38	189	59.46	4.12
39	275	59.46	4.12
40	213	20.31	2.62
41	213	20.31	0.02
42	213	20.31	2.60
43	275	59.46	1.50
44	630	20.03	18.19

	t (C)	p (bar)	m (kg/s)
45	700	20.00	26.06
46	700	20.00	16.69
47	700	20.00	1.50
48	247	1.00	7.87
49	150	1.00	7.83
50	25	20.00	4.26
51	25	20.00	6.71
52	140	20.00	7.74
53	25	20.00	2.45
54	140	20.00	1.19
55	140	20.00	44.87
56	170	20.31	46.72
57	140	20.31	43.68

* the gasifier flowsheet can be seen on the previous figure (on wood pellets).